Supporting Information: Ab Initio Nonadiabatic Molecular Dynamics with Hole-Hole Tamm-Dancoff Approximated Density Functional Theory

Jimmy K. Yu,[*,†,‡,¶] Christoph Bannwarth,[*,†,‡] Edward G. Hohenstein,[*,†,‡] and Todd J. Martínez[*,†,‡]

†*Department of Chemistry and The PULSE Institute, Stanford University, Stanford, CA 94305, United States of America.*

‡*SLAC National Accelerator Laboratory, 2575 Sand Hill Road, Menlo Park, CA 94025, United States of America.*

¶*Biophysics Program, Stanford University, Stanford, CA 94305, United States of America.*

E-mail: jkyu@stanford.edu; cbannwarth@posteo.net; egh4@stanford.edu; toddjmartinez@gmail.com

Contents

List of Tables **S-2**

1 Benchmarking vertical excitation energies at the Franck-Condon point with *hh*-TDA **S-4**

1.1 Intermolecular charge-transfer set S-4

1.2 Push-pull-type set S-7

1.3 Local excitation set S-9

1.4 State-splittings S-12

1.5 Standard *hh*-TDA vs FOMO-*hh*-TDA S-15

2 Additional Details for Azobenzene Studies **S-17**

2.1 Dihedral scans S-17

2.2 Azobenzene AIMS-FOMO-*hh*-TDA-BHLYP/def2-SVP dynamics with d-functions excluded S-20

References **S-23**

List of Tables

S1 Considered mean field electronic structure methods S-4

S2 Detailed results for global hybrids on the CT set S-5

S3 Detailed results for range-separated functionals on the CT set S-6

S4 Detailed results for global hybrids on the intramolecular CT set S-8

S5 Detailed results for range-separated hybrids on the intramolecular CT set . . S-9

S6 Detailed results for global hybrids on the local excitation set S-11

S7 Detailed results for range-sparated hybrids on the local excitation set S-12

S8 Detailed results for global hybrids on the state splitting set S-13

S9 Detailed results for range-separated hybrids on the state splitting set S-14

1 Benchmarking vertical excitation energies at the Franck-Condon point with *hh*-TDA

Here, we benchmark FOMO-*hh*-TDA in combination with common density functional approximations (DFAs) along with Hartree-Fock (HF) in the calculation of vertical excitation energies for different excitation types (see below). The functionals used are given in Table S1. All FOMO-*hh*-TDA calculations are carried out with a development version of the GPU-accelerated electronic structure code TeraChem.[S1,S2] For each DFA, the SCF calculation is performed for an N-electron reference with constant fractional occupation of $n_i = \frac{N}{\frac{N}{2}+1}$, $\forall\, i \in [1, \frac{N}{2}+1]$. The *hh*-TDA step is then performed on the entire space of the lowest $\frac{N}{2}+1$ orbitals following convergence for the SCF procedure.

Table S1: Mean field electronic structure methods considered in the benchmarking and the amount of short- and long-range Fock exchange and the range-sparation parameter ω value (if applicable) corresponding to each.

Method	c_{HF} $(r_{12}=0)$	c_{HF} $(r_{12}=\infty)$	ω
Hartree-Fock (HF)	1.00	1.00	n.a.
B3LYP	0.20	0.20	n.a.
PBE0	0.25	0.25	n.a.
BHLYP	0.50	0.50	n.a.
CAM-B3LYP	0.19	0.65	0.33
ωB97	0.00	1.00	0.40
ωB97X	0.157706	1.00	0.30
ωB97X-D3	0.195728	1.00	0.25
ωPBEh	0.20	1.00	0.20

We consider the same benchmarks previously used in Ref. S3 with reference data from Refs. S4–S6. The individual benchmark sets are discussed below.

1.1 Intermolecular charge-transfer set

The intermolecular charge-transfer set is from Ref. S4. The CT states are identified as excitations for which the change in the static dipole moment exceeds 8 Debye.

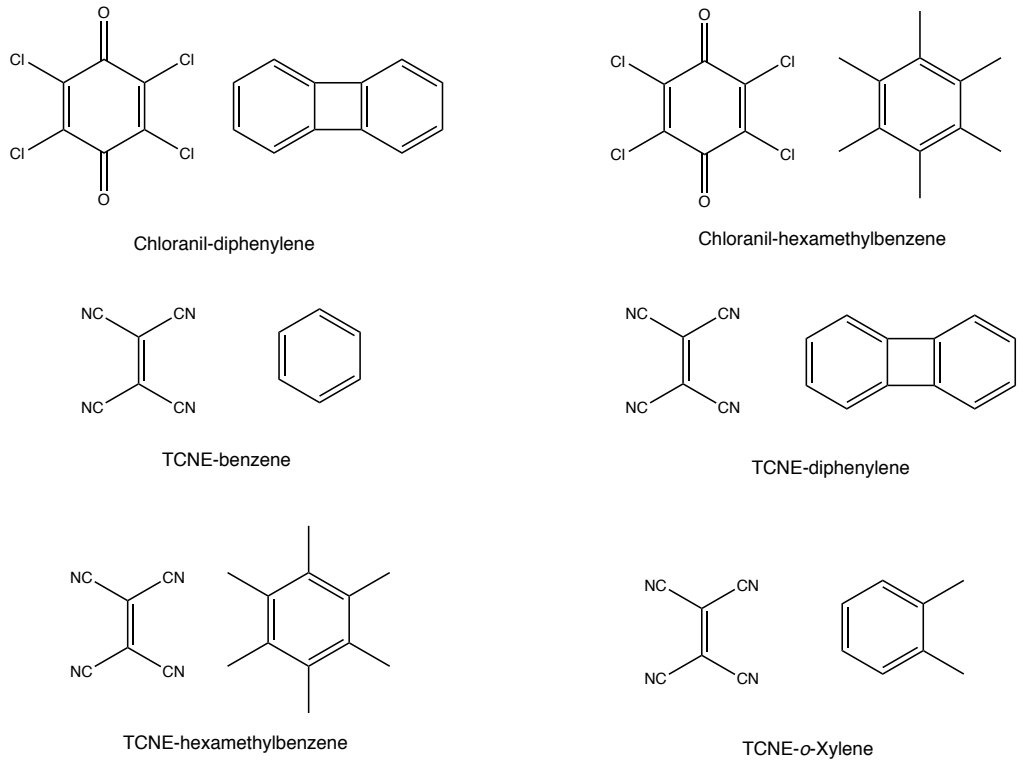

Figure S1: Molecules considered in the intermolecular charge-transfer set. TCNE: tetracyanoethylene.

Table S2: Vertical excitations computed with FOMO-*hh*-TDA for molecules with charge-transfer-type excitations (set taken from Ref. S4). Hartree Fock and different global hybrid functionals are considered and the spherical def2-SV(P)[S7,S8] basis set is used throughout. The excitation energies are given in eV (dimensionless oscillator strength in parentheses). If the state of interest is not S_1, it is also denoted in parentheses.

system	B3LYP	PBE0	BHLYP	HF	ref.[a]
Chloranil-diphenylene	3.82 (0.030, S_4)	4.15 (0.033, S_5)	3.39 (0.051)	2.01 (0.127)	2.81
Chloranil-hexamethylbenzene	4.09 (0.029, S_5)	3.94 (0.031, S_4)	3.14 (0.000)	2.03 (0.000)	2.87
TCNE-benzene	5.13 (0.000, S_2)	5.00 (0.000, S_2)	4.23 (0.000)	2.63 (0.000)	3.78
TCNE-diphenylene	2.90 (0.005)	2.94 (0.006)	2.72 (0.010)	0.93 (0.051)	2.28
TCNE-hexamethylbenzene	3.26 (0.001)	3.15 (0.000)	2.44 (0.000)	1.08 (0.000)	2.36
TCNE-*o*-xylene	4.32 (0.013, S_2)	4.20 (0.013, S_2)	3.44 (0.012)	1.90 (0.020)	3.17
MD:	1.04	1.02	0.35	−1.11	–
MAD:	1.04	1.02	0.35	1.11	–
RMSD:	1.07	1.05	0.38	1.14	–
SD:	0.26	0.26	0.18	0.24	–
MAX:	1.35	1.34	0.58	1.36	–

[a] SCS-CC2/def2-TZVP(-f) from Ref. S4. TCNE: Tetracyanoethylene.

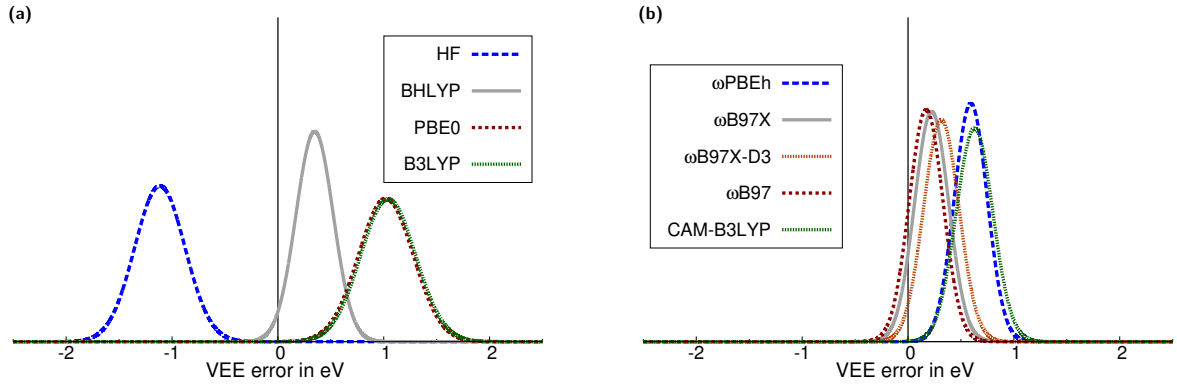

Figure S2: Gaussian error distribution functions for FOMO-*hh*-TDA with different standard density functionals in the calculation of intermolecular charge-transfer (CT) excitation energies. The spherical def2-SV(P)[S7,S8] basis set is used throughout. The center of the Gaussian corresponds to the mean deviation (MD), while the width of the Gaussian corresponds to the standard deviation (SD) for the vertical excitation energies on the CT set (see Tables S2 and S3 for details).

Table S3: Vertical excitations computed with FOMO-*hh*-TDA for different molecules with charge-transfer-type excitations (set taken from Ref. S4). Different range-separated hybrid functionals are considered and the spherical def2-SV(P)[S7,S8] basis set is used throughout. The excitation energies are given in eV (dimensionless oscillator strength in parentheses). If the state of interest is not S_1, it is also denoted in parentheses.

system	CAM-B3LYP	ωPBEh	ωB97	ωB97X	ωB97X-D3	ref.[a]
Chloranil-diphenylene	3.61 (0.048, S_4)	3.53 (0.048, S_4)	3.17 (0.070, S_2)	3.21 (0.063, S_2)	3.29 (0.057, S_3)	2.81
Chloranil-hexamethylbenzene	3.49 (0.041, S_4)	3.41 (0.040, S_4)	2.97 (0.000)	2.98 (0.000)	3.03 (0.000, S_2)	2.87
TCNE-benzene	4.54 (0.000, S_2)	4.53 (0.029, S_2)	4.12 (0.000)	4.18 (0.000)	4.28 (0.000)	3.78
TCNE-diphenylene	2.99 (0.009)	2.95 (0.010)	2.44 (0.018)	2.52 (0.016)	2.65 (0.014)	2.28
TCNE-hexamethylbenzene	2.69 (0.000)	2.69 (0.000)	2.30 (0.000)	2.36 (0.000)	2.45 (0.000)	2.36
TCNE-*o*-xylene	3.73 (0.012)	3.71 (0.012)	3.30 (0.015)	3.36 (0.015)	3.46 (0.014)	3.17
MD:	0.63	0.59	0.17	0.22	0.31	–
MAD:	0.63	0.59	0.19	0.22	0.31	–
RMSD:	0.65	0.61	0.22	0.27	0.35	–
SD:	0.17	0.16	0.16	0.16	0.17	–
MAX:	0.80	0.75	0.36	0.40	0.50	–

[a] SCS-CC2/def2-TZVP(-f) from Ref. S4. TCNE: Tetracyanoethylene.

1.2 Push-pull-type set

The push-pull-type excitation benchmark set is a subset of geometries, as classified in Ref. S3, and their corresponding reference excitation energies taken from Refs. S4 and S5. The considered molecules are given in Fig. S1.

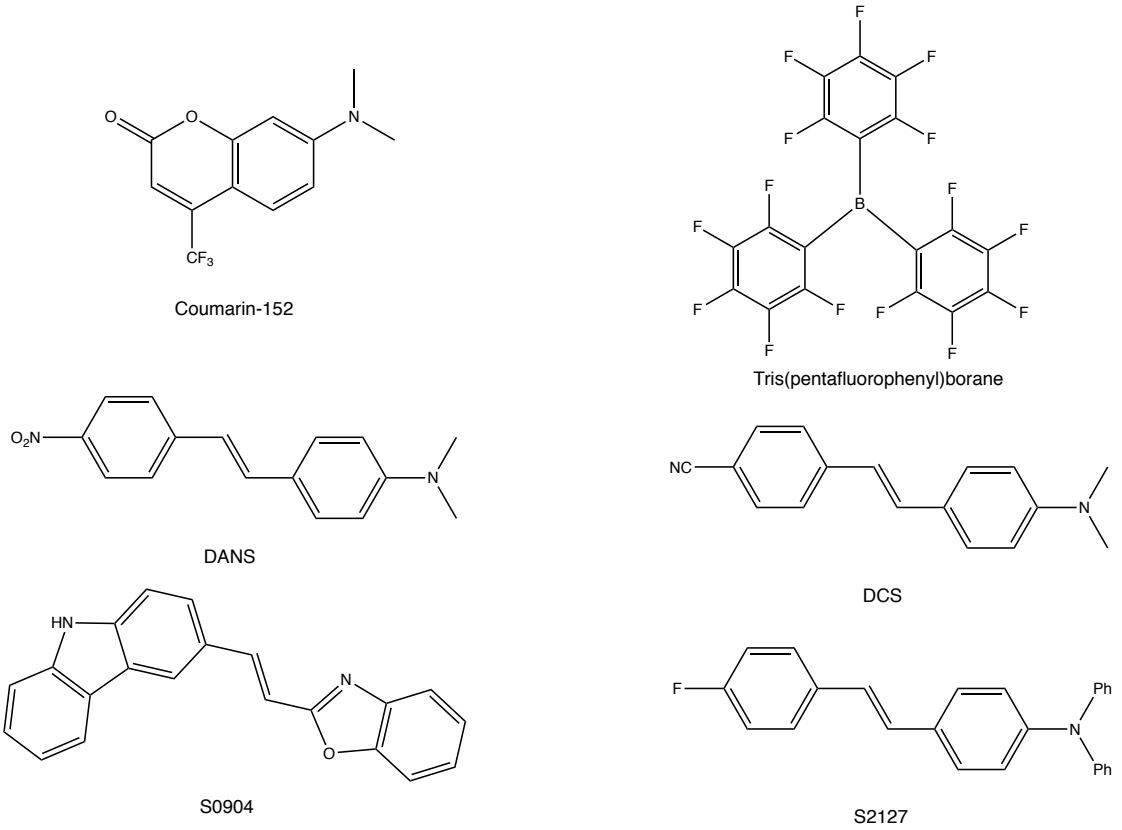

Figure S3: Molecules considered in the mixed intramolecular charge-transfer set. DANS: 4-Dimethylamino-4'-nitrostilbene, DCS: 4-Dimethylamino-4'-cyanostilbene, S0904: (*E*)-1-(2-Carbazyl)-2-(2-benzoxazyl)-ethylene, S2127: 4-Diphenylamino-4'-fluorostilbene.

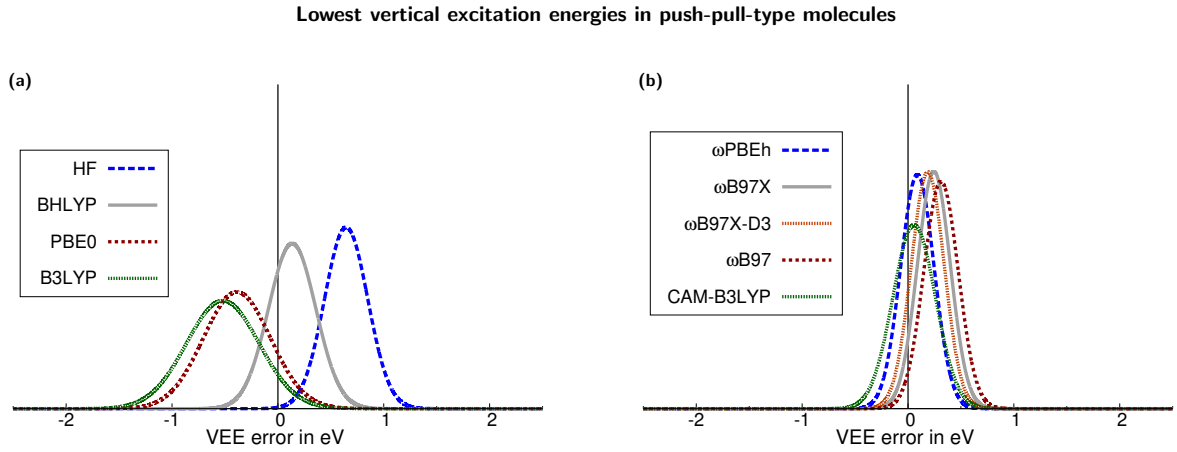

Figure S4: Gaussian error distribution functions for FOMO-*hh*-TDA with different standard density functionals in the calculation of vertical push-pull-type excitation energies. The spherical def2-SV(P)[S7,S8] basis set is used throughout. The center of the Gaussian corresponds to the mean deviation (MD) and the width of the Gaussian corresponds to the standard deviation (SD) for the vertical excitation energies on the push-pull set (see Tables S4 and S5 for details).

Table S4: Vertical excitations computed with FOMO-*hh*-TDA for molecules with partial intramolecular charge-transfer-type excitations (systems taken from Ref. S4 and S5). Hartree Fock and different global hybrid functionals are considered and the spherical def2-SV(P)[S7,S8] basis set is used throughout. The values are given in eV (dimensionless oscillator strength in parentheses). If not denoted otherwise, the reference values are taken from Ref. S4.

system	B3LYP	PBE0	BHLYP	HF	ref.[a]
$B(C_6F_6)_3$	4.08 (0.285)	4.17 (0.274)	4.56 (0.112)	4.86 (0.096)	4.10[b]
Coumarin-152	3.53 (0.911)	3.65 (0.968)	4.07 (1.188)	4.63 (1.470)	3.69
DANS	2.77 (1.871)	2.90 (2.009)	3.39 (2.502)	3.82 (2.782)	3.42
DCS	2.81 (1.858)	2.94 (1.999)	3.49 (2.562)	4.18 (3.136)	3.56
S0904	3.12 (1.332)	3.27 (1.499)	3.83 (2.266)	4.25 (2.992)	3.81[b]
S2127	2.81 (1.158)	2.99 (1.325)	3.72 (1.941)	4.37 (2.152)	3.66[b]
MD:	−0.52	−0.39	0.14	0.64	–
MAD:	0.52	0.41	0.17	0.64	–
RMSD:	0.61	0.48	0.24	0.67	–
SD:	0.34	0.32	0.22	0.20	–
MAX:	0.85	0.67	0.46	0.94	–

[a] SCS-CC2/def2-TZVP(-f) from Ref. S4. [b] SCS-CC2/aug-cc-pVDZ from Ref. S5. DANS: 4-Dimethylamino-4'-nitrostilbene, DCS: 4-Dimethylamino-4'-cyanostilbene, S0904: (*E*)-1-(2-Carbazyl)-2-(2-benzoxazyl)-ethylene , S2127: 4-Diphenylamino-4'-fluorostilbene.

Table S5: Vertical excitations computed with FOMO-*hh*-TDA for molecules with partial intramolecular charge-transfer-type excitations (set taken from Ref. S4 and S5). Different range-separated hybrid functionals are considered and the spherical def2-SV(P)[S7,S8] basis set is used throughout. The excitation energies are given in eV (dimensionless oscillator strength in parentheses). If not denoted otherwise, the reference values are taken from Ref. S4.

system	CAM-B3LYP	ωPBEh	ωB97	ωB97X	ωB97X-D3	ref.[a]
$B(C_6F_6)_3$	4.43 (0.109)	4.37 (0.104)	4.53 (0.100)	4.49 (0.101)	4.45 (0.102)	4.10[b]
Coumarin-152	3.99 (1.205)	3.99 (1.247)	4.27 (1.408)	4.17 (1.355)	4.09 (1.314)	3.69
DANS	3.36 (2.575)	3.41 (2.635)	3.62 (2.804)	3.55 (2.720)	3.49 (2.680)	3.42
DCS	3.41 (2.615)	3.47 (2.697)	3.71 (3.006)	3.64 (2.884)	3.57 (2.807)	3.56
S0904	3.77 (2.295)	3.83 (2.439)	4.02 (2.775)	3.97 (2.675)	3.92 (2.591)	3.81[b]
S2127	3.64 (2.027)	3.71 (2.142)	3.96 (2.360)	3.90 (2.269)	3.83 (2.223)	3.66[b]
MD:	0.06	0.09	0.31	0.24	0.19	–
MAD:	0.15	0.12	0.31	0.24	0.19	–
RMSD:	0.19	0.17	0.35	0.28	0.23	–
SD:	0.20	0.16	0.16	0.16	0.16	–
MAX:	0.33	0.30	0.58	0.48	0.40	–

[a] SCS-CC2/def2-TZVP(-f) from Ref. S4. [b] SCS-CC2/aug-cc-pVDZ from Ref. S5. DANS: 4-Dimethylamino-4'-nitrostilbene, DCS: 4-Dimethylamino-4'-cyanostilbene, S0904: (*E*)-1-(2-Carbazyl)-2-(2-benzoxazyl)-ethylene , S2127: 4-Diphenylamino-4'-fluorostilbene.

1.3 Local excitation set

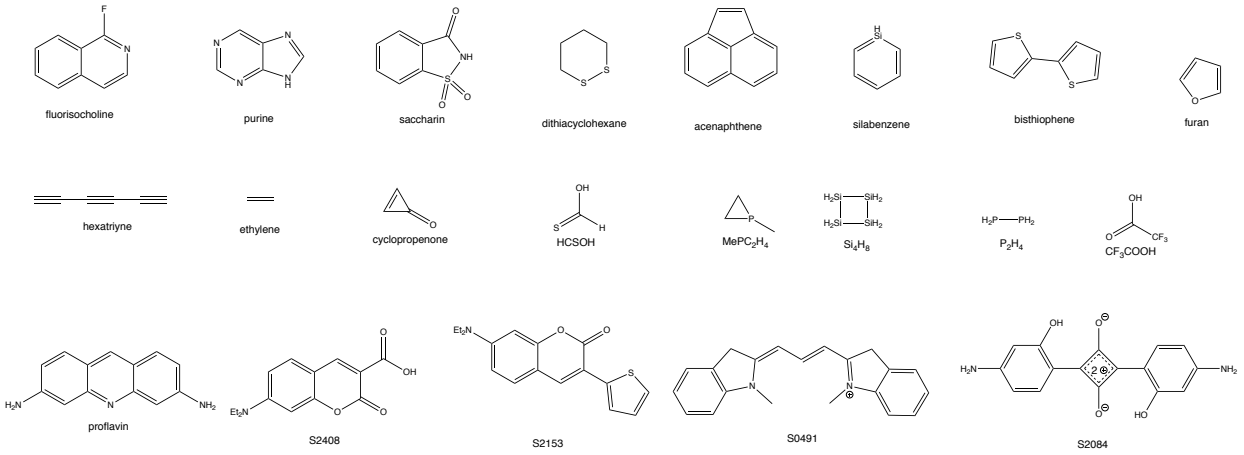

Figure S5: Molecules considered in the local excitation set. S2408: 7-diethylamino-2-oxo-2H-chromene-3-carboxylic acid. S0491: 1-methyl-indole based Cy3 dye. S2153: 7-diethylamino-3-thiophen-2-yl-chromen-2-one S2084: 1,3-bis[4-amino-2-hydroxyphenyl]-2,4-dioxy-cyclobutene

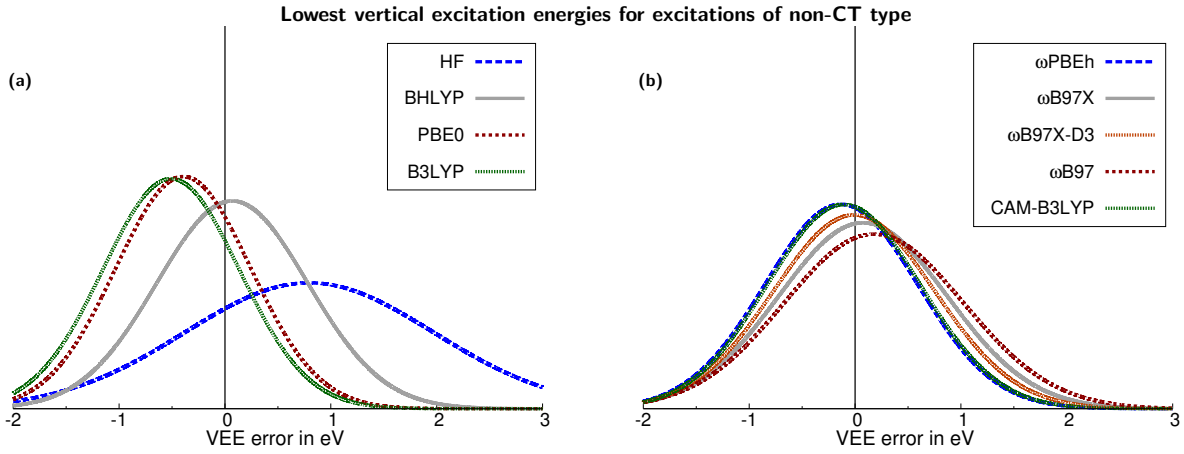

Figure S6: Gaussian error distribution functions for FOMO-*hh*-TDA with different standard density functionals in the calculation of lowest vertical excitation energies with no (or little) charge-transfer character. The spherical def2-SV(P)[S7,S8] basis set is used throughout. The center of the Gaussian corresponds to the mean deviation (MD) and the width of the Gaussian corresponds to the standard deviation (SD) for the vertical excitation energies on the non-CT set (see Tables S6 and S7 for details).

Table S6: Lowest vertical excitations computed with FOMO-*hh*-TDA for different molecules with predominantly local lowest vertical excitations (unless noted otherwise, systems are taken from Ref. S5). Hartree Fock and different global hybrid functionals are considered and the spherical def2-SV(P)[S7,S8] basis set is used throughout. The excitation energies are given in eV (dimensionless oscillator strength in parentheses). If the state of interest is not S_1, it is also denoted in parentheses.

system	B3LYP	PBE0	BHLYP	HF	ref.[a]
Acenaphthylene	2.60 (0.004)	2.71 (0.004)	3.13 (0.002)	3.89 (0.003)	3.65 (0.000)
Bisthiophen	3.55 (0.736)	3.72 (0.794)	4.35 (1.054)	5.47 (1.538)	4.48 (0.395)
CF_3COOH	6.25 (0.015)	6.32 (0.016)	6.53 (0.011)	6.81 (0.007)	5.95 (0.000)
Cyclopropenon	2.26 (0.005)	2.22 (0.004)	1.94 (0.003)	1.59 (0.002)	4.42 (0.000)
Dithiacyclohexan	4.72 (0.021)	4.79 (0.019)	4.92 (0.013)	5.02 (0.007)	4.52 (0.009)
Ethylene	5.79 (0.455)	6.10 (0.464)	7.64 (0.496)	10.81 (0.556, S_3)	7.80 (0.410)[b]
Fluorisochinolin	4.24 (0.468)	4.40 (0.478)	5.05 (0.519)	6.06 (0.574)	4.50 (0.028)
Furan	5.84 (0.356)	5.96 (0.359)	6.53 (0.366)	8.18 (0.425)	6.32 (0.159)[b]
HCSOH	3.68 (0.000)	3.65 (0.000)	3.31 (0.000)	2.99 (0.000)	3.57 (0.000)
Hexatriyne	3.84 (0.000)	3.94 (0.000)	4.15 (0.000)	4.54 (0.000)	4.85 (0.000)
$MePC_2H_4$	6.20 (0.237)	6.38 (0.235)	6.95 (0.215)	7.85 (0.145)	6.53 (0.040)
P_2H_4	6.34 (0.850)	6.52 (0.820)	7.20 (0.731)	6.53 (0.003)	6.25 (0.050)
Proflavin	2.98 (0.238)	3.11 (0.236)	3.63 (0.227)	4.32 (0.175)	3.54 (0.234)
Purine	4.18 (0.001)	4.29 (0.001)	5.05 (0.001)	6.37 (0.002)	4.69 (0.003)
S0491	2.65 (1.674)	2.76 (1.772)	3.10 (2.004)	2.98 (1.903)	2.70 (1.548)
S2084	2.24 (1.370)	2.34 (1.484)	2.69 (1.980)	3.36 (2.629)	2.37 (1.423)
S2153	3.05 (1.404)	3.17 (1.503)	3.63 (1.873)	4.21 (2.357)	3.48 (1.004)
S2408	3.37 (1.329)	3.50 (1.402)	4.01 (1.669)	4.92 (2.068)	3.64 (0.838)
Saccharin	4.68 (0.004)	4.80 (0.004)	5.47 (0.004)	6.55 (0.005)	4.91 (0.004)
Si_4H_8	4.55 (0.000)	4.58 (0.000)	4.96 (0.000)	5.65 (0.000)	5.22 (0.000)
Silabenzene	3.92 (0.477)	4.09 (0.493)	4.82 (0.564)	6.25 (0.706)	4.23 (0.059)
MD:	−0.51	−0.39	0.07	0.80	–
MAD:	0.58	0.49	0.50	1.15	–
RMSD:	0.81	0.74	0.70	1.40	–
SD:	0.64	0.64	0.71	1.17	–
MAX:	2.16	2.20	2.48	3.01	–

[a] Structures and reference values (SCS-CC2/aug-cc-pVXZ (X=D,T)) from Ref. S5. [b] Best estimate energy value from Ref. S6 (CCSD value for oscillator strength).

Table S7: Lowest vertical excitations computed with FOMO-*hh*-TDA for different molecules with predominantly local lowest vertical excitations (unless noted otherwise, systems are taken from Ref. S5). Different range-sparated hybrid functionals are considered and the spherical def2-SV(P)[S7,S8] basis set is used throughout. The excitation energies are given in eV (dimensionless oscillator strength in parentheses).

system	CAM-B3LYP	ωPBEh	ωB97	ωB97X	ωB97X-D3	ref.[a]
Acenaphthylene	3.08 (0.012)	3.10 (0.012)	3.46 (0.026)	3.35 (0.019)	3.25 (0.015)	3.65 (0.000)
Bisthiophen	4.19 (1.033)	4.23 (1.054)	4.66 (1.286)	4.54 (1.209)	4.42 (1.147)	4.48 (0.395)
CF_3COOH	6.36 (0.014)	6.32 (0.016)	6.44 (0.016)	6.39 (0.015)	6.36 (0.015)	5.95 (0.000)
Cyclopropenon	1.88 (0.003)	1.98 (0.004)	1.52 (0.002)	1.68 (0.003)	1.80 (0.003)	4.42 (0.000)
Dithiacyclohexan	4.94 (0.016)	4.95 (0.017)	5.13 (0.014)	5.05 (0.014)	5.01 (0.015)	4.52 (0.009)
Ethylene	6.49 (0.487)	6.28 (0.480)	6.80 (0.520)	6.71 (0.503)	6.55 (0.492)	7.80 (0.410)[b]
Fluorisochinolin	4.78 (0.506)	4.73 (0.498)	5.17 (0.542)	5.05 (0.524)	4.92 (0.513)	4.50 (0.028)
Furan	6.21 (0.369)	6.14 (0.369)	6.57 (0.394)	6.39 (0.380)	6.28 (0.374)	6.32 (0.159)[b]
HCSOH	3.64 (0.000)	3.69 (0.000)	3.82 (0.000)	3.69 (0.000)	3.66 (0.000)	3.57 (0.000)
Hexatriyne	4.15 (0.000)	4.18 (0.000)	4.45 (0.000)	4.33 (0.000)	4.25 (0.000)	4.85 (0.000)
$MePC_2H_4$	6.70 (0.243)	6.63 (0.243)	7.10 (0.250)	6.93 (0.244)	6.80 (0.243)	6.53 (0.040)
P_2H_4	7.02 (0.822)	6.95 (0.817)	7.50 (0.736)	7.33 (0.775)	7.17 (0.801)	6.25 (0.050)
Proflavin	3.45 (0.224)	3.40 (0.204)	3.73 (0.198)	3.63 (0.196)	3.54 (0.199)	3.54 (0.234)
Purine	4.69 (0.001)	4.56 (0.001)	5.04 (0.002)	4.89 (0.001)	4.77 (0.001)	4.69 (0.003)
S0491	3.17 (2.043)	3.22 (2.089)	3.34 (2.085)	3.29 (2.076)	3.26 (2.078)	2.70 (1.548)
S2084	2.72 (1.932)	2.84 (2.076)	3.08 (2.318)	3.00 (2.271)	2.94 (2.209)	2.37 (1.423)
S2153	3.55 (1.887)	3.59 (1.973)	3.86 (2.243)	3.77 (2.154)	3.69 (2.082)	3.48 (1.004)
S2408	3.92 (1.689)	3.93 (1.738)	4.31 (1.924)	4.17 (1.861)	4.07 (1.814)	3.64 (0.838)
Saccharin	4.99 (0.004)	4.86 (0.004)	5.08 (0.004)	5.04 (0.004)	4.98 (0.004)	4.91 (0.004)
Si_4H_8	4.94 (0.000)	4.85 (0.000)	5.26 (0.000)	5.13 (0.000)	5.02 (0.000)	5.22 (0.000)
Silabenzene	4.53 (0.560)	4.47 (0.555)	5.01 (0.641)	4.84 (0.608)	4.69 (0.586)	4.23 (0.059)
MD:	−0.11	−0.13	0.18	0.07	−0.01	–
MAD:	0.46	0.47	0.60	0.53	0.48	–
RMSD:	0.71	0.72	0.84	0.78	0.74	–
SD:	0.72	0.72	0.85	0.80	0.76	–
MAX:	2.54	2.44	2.90	2.74	2.62	–

[a] Structures and reference values (SCS-CC2/aug-cc-pVXZ (X=D,T)) from Ref. S5. [b] Best estimate energy value from Ref. S6 (CCSD value for oscillator strength).

1.4 State-splittings

In the state-splitting set below, two states are included for each molecule. The only exception is pyrimidine for which four states are considered. This set is mostly based on Thiel's benchmark[S6] and was collected in Ref. S3.

Table S8: Vertical excitation energies computed with FOMO-*hh*-TDA for different states on small molecule. Unless noted otherwise, systems are taken from Ref. S6. Hartree Fock and different global hybrid functionals are considered and the spherical def2-SV(P)[S7,S8] basis set has been used throughout. The excitation energies are given in eV (dimensionless oscillator strength in parentheses).

system	state		B3LYP	PBE0	BHLYP	HF	ref.[a]
Acetamide	1^1A"	$n \to \pi^*$	4.93 (0.003)	5.08 (0.003)	5.36 (0.003)	–[b]	5.80 (0.001)
	$2^1A'$	$\pi \to \pi^*$	6.93 (0.485)	7.21 (0.489)	7.95 (0.473)	–[b]	7.27 (0.223)
Acetone	1^1A_2	$n \to \pi^*$	3.65 (0.000)	3.80 (0.000)	4.09 (0.000)	4.25 (0.000)	4.40 (0.000)
	2^1A_1	$\pi \to \pi^*$	7.36 (0.567)	7.79 (0.584)	9.35 (0.624)	10.72 (0.271)	9.40 (0.256)
Adenine	1^1A"	$n \to \pi^*$	4.92 (0.000)	5.07 (0.000)	5.90 (0.000)	7.41 (0.001)	5.12 (0.001)
	$3^1A'$	$\pi \to \pi^*$	4.52 (0.645)	4.71 (0.674)	5.50 (0.786)	7.01 (1.018)	5.25 (0.297)
Aspirin	2^1A	$\pi \to \pi^*$	4.77 (0.366)	4.96 (0.381)	5.73 (0.269)	6.48 (0.388)	4.80 (0.022)[c]
	3^1A	$n/\pi \to \pi^*$	4.49 (0.026)	4.66 (0.027)	5.48 (0.138)	6.85 (0.052)	5.36 (0.001)[c]
Cyclopentadiene	1^1B_2	$\pi \to \pi^*$	3.88 (0.191)	4.10 (0.201)	5.04 (0.239)	6.85 (0.332)	5.55 (0.097)
	2^1A_1	$\pi \to \pi^*$	6.22 (0.455)	6.41 (0.446)	6.98 (0.364)	7.99 (0.328)	6.31 (0.648)
Cyclopropene	1^1B_1	$\sigma \to \pi^*$	6.35 (0.000)	6.45 (0.013)	6.84 (0.000)	5.97 (0.007)	6.76 (0.001)
	1^1B_2	$\pi \to \pi^*$	5.63 (0.371)	5.90 (0.370)	7.08 (0.344)	7.52 (0.000)	7.06 (0.083)
Cytosine	$2^1A'$	$\pi \to \pi^*$	4.82 (0.246)	4.91 (0.240)	5.11 (0.208)	5.33 (0.143)	4.66 (0.058)
	1^1A"	$n \to \pi^*$	4.88 (0.000)	4.95 (0.000)	5.25 (0.000)	5.63 (0.000)	4.87 (0.002)
Formaldehyde	1^1A_2	$n \to \pi^*$	3.42 (0.000)	3.48 (0.000)	3.69 (0.000)	3.65 (0.000)	3.88 (0.000)
	2^1A_1	$\pi \to \pi^*$	8.21 (0.465)	8.48 (0.463)	9.38 (0.050)	11.13 (0.003)	9.30 (0.374)
Formamide	1^1A"	$n \to \pi^*$	5.44 (0.001)	5.48 (0.002)	5.48 (0.002)	6.00 (0.001)	5.63 (0.001)
	$2^1A'$	$\pi \to \pi^*$	7.45 (0.564)	7.66 (0.567)	8.23 (0.556)	6.64 (0.458)	7.44 (0.371)
Imidazole	$2^1A'$	$\pi \to \pi^*$	6.02 (0.358)	6.19 (0.367)	6.84 (0.389)	–[b]	6.19 (0.088)
	1^1A"	$n \to \pi^*$	6.31 (0.003)	6.40 (0.003)	6.79 (0.003)	–[b]	6.81 (0.005)
Norbornadiene	1^1A_2	$\pi \to \pi^*$	4.05 (0.000)	4.23 (0.000)	5.06 (0.000)	6.62 (0.000)	5.34 (0.000)
	1^1B_2	$\pi \to \pi^*$	5.04 (0.290)	5.22 (0.288)	6.14 (0.286)	7.76 (0.259)	6.11 (0.029)
p-Benzoquinone	1^1B_{1g}	$n \to \pi^*$	2.14 (0.000)	2.21 (0.000)	2.80 (0.000)	3.77 (0.000)	2.78 (0.000)
	1^1B_{1u}	$\pi \to \pi^*$	5.80 (0.001)	4.44 (1.385)	5.42 (1.537)	7.05 (1.811)	5.29 (0.558)
Propanamide	1^1A"	$n \to \pi^*$	4.88 (0.004)	5.05 (0.004)	5.43 (0.004)	–[b]	5.72 (0.001)
	$2^1A'$	$\pi \to \pi^*$	6.79 (0.460)	7.09 (0.466)	7.92 (0.454)	–[b]	7.20 (0.108)
Pyrazine	1^1B_{3u}	$n \to \pi^*$	4.08 (0.007)	4.12 (0.007)	4.42 (0.007)	4.99 (0.007)	3.95 (0.008)
	1^1B_{2u}	$\pi \to \pi^*$	5.95 (0.460)	6.00 (0.474)	6.12 (0.511)	6.67 (0.578)	4.64 (0.067)
Pyridazine	1^1B_1	$n \to \pi^*$	3.14 (0.007)	3.25 (0.007)	3.82 (0.008)	4.70 (0.009)	3.78 (0.007)
	2^1A_1	$\pi \to \pi^*$	6.02 (0.556)	6.14 (0.571)	6.58 (0.622)	7.72 (0.725)	5.18 (0.014)
Pyridine	1^1B_1	$n \to \pi^*$	4.34 (0.004)	4.46 (0.004)	4.99 (0.004)	5.81 (0.005)	4.59 (0.006)
	1^1B_2	$\pi \to \pi^*$	5.89 (0.483)	5.99 (0.497)	6.28 (0.537)	7.05 (0.615)	4.85 (0.022)
Pyrimidine	1^1B_1	$n \to \pi^*$	4.19 (0.007)	4.27 (0.007)	4.74 (0.007)	5.47 (0.008)	4.55 (0.007)
	1^1A_2	$n \to \pi^*$	5.70 (0.000)	5.82 (0.000)	6.31 (0.000)	7.09 (0.000)	4.91 (0.000)
	1^1B_2	$\pi \to \pi^*$	6.17 (0.554)	6.29 (0.568)	6.75 (0.622)	7.84 (0.736)	5.44 (0.022)
	2^1A_1	$\pi \to \pi^*$	6.28 (0.509)	6.50 (0.519)	7.38 (0.546)	8.88 (0.600)	6.95 (0.038)
s-Tetrazine	1^1B_{3u}	$n \to \pi^*$	2.52 (0.011)	2.54 (0.011)	2.86 (0.011)	3.31 (0.012)	2.24 (0.009)
	1^1A_u	$\pi \to \pi^*$	5.84 (0.000)	5.90 (0.000)	6.10 (0.000)	6.39 (0.000)	3.48 (0.000)
Thymine	1^1A"	$n \to \pi^*$	4.88 (0.003)	4.96 (0.003)	5.31 (0.002)	5.78 (0.001)	4.82 (0.000)
	$2^1A'$	$\pi \to \pi^*$	4.92 (0.685)	5.08 (0.710)	5.74 (0.774)	6.49 (0.343)	5.20 (0.222)
Uracil	1^1A"	$n \to \pi^*$	4.79 (0.003)	4.86 (0.003)	5.18 (0.002)	5.54 (0.001)	4.80 (0.000)
	$2^1A'$	$\pi \to \pi^*$	5.00 (0.668)	5.17 (0.693)	5.79 (0.789)	6.45 (0.225)	5.35 (0.224)
		MD:	−0.25	−0.14	0.43	1.13	–
		MAD:	0.64	0.57	0.54	1.29	–
		RMSD:	0.84	0.77	0.75	1.46	–
		SD:	0.81	0.76	0.62	0.94	–
		MAX:	2.36	2.42	2.62	2.91	–

[a] Best estimate energy value from Ref. S6 (CCSD value for oscillator strength). [b] A σ^* orbital is populated in the SCF calculation instead of the π^* orbital, hence no comparison is made. [c] Structure and reference values (SCS-CC2/aug-cc-pVDZ) from Ref. S5.

Table S9: Vertical excitation energies computed with FOMO-*hh*-TDA for different states on small molecule. Unless noted otherwise, systems are taken from Ref. S6. Different range-separated hybrid functionals are considered and the spherical def2-SV(P)[S7,S8] basis set is used throughout. The excitation energies are given in eV (dimensionless oscillator strength in parentheses).

system	state		CAM-B3LYP	ωPBEh	ωB97	ωB97X	ωB97X-D3	ref.[a]
Acetamide	1^1A"	$n \rightarrow \pi^*$	5.26 (0.003)	5.23 (0.003)	5.54 (0.003)	5.41 (0.003)	5.33 (0.003)	5.80 (0.001)
	$2^1A'$	$\pi \rightarrow \pi^*$	7.48 (0.511)	7.41 (0.513)	7.73 (0.556)	7.69 (0.530)	7.60 (0.521)	7.27 (0.223)
Acetone	1^1A_2	$n \rightarrow \pi^*$	3.98 (0.000)	3.94 (0.000)	4.21 (0.000)	4.11 (0.000)	4.05 (0.000)	4.40 (0.000)
	2^1A_1	$\pi \rightarrow \pi^*$	8.14 (0.623)	8.00 (0.615)	8.32 (0.679)	8.38 (0.648)	8.27 (0.631)	9.40 (0.256)
Adenine	1^1A"	$n \rightarrow \pi^*$	5.56 (0.000)	5.45 (0.000)	6.06 (0.000)	5.86 (0.000)	5.70 (0.000)	5.12 (0.001)
	$3^1A'$	$\pi \rightarrow \pi^*$	5.30 (0.795)	5.29 (0.798)	5.93 (0.926)	5.73 (0.881)	5.55 (0.847)	5.25 (0.297)
Aspirin	2^1A	$\pi \rightarrow \pi^*$	5.44 (0.425)	5.40 (0.429)	5.87 (0.460)	5.73 (0.440)	5.60 (0.435)	4.80 (0.022)[b]
	3^1A	$n/\pi \rightarrow \pi^*$	5.04 (0.020)	4.90 (0.009)	5.20 (0.008)	5.14 (0.009)	5.07 (0.010)	5.36 (0.001)[b]
Cyclopentadiene	1^1B_2	$\pi \rightarrow \pi^*$	4.42 (0.224)	4.30 (0.217)	4.76 (0.257)	4.64 (0.242)	4.51 (0.231)	5.55 (0.097)
	2^1A_1	$\pi \rightarrow \pi^*$	6.75 (0.400)	6.69 (0.424)	7.21 (0.388)	7.01 (0.391)	6.87 (0.400)	6.31 (0.648)
Cyclopropene	1^1B_1	$\sigma \rightarrow \pi^*$	6.65 (0.000)	6.63 (0.000)	6.66 (0.011)	6.80 (0.000)	6.69 (0.000)	6.76 (0.001)
	1^1B_2	$\pi \rightarrow \pi^*$	6.14 (0.373)	5.99 (0.373)	6.30 (0.377)	6.27 (0.372)	6.17 (0.372)	7.06 (0.083)
Cytosine	$2^1A'$	$\pi \rightarrow \pi^*$	4.89 (0.206)	4.85 (0.204)	4.84 (0.174)	4.84 (0.182)	4.85 (0.191)	4.66 (0.058)
	1^1A"	$n \rightarrow \pi^*$	5.04 (0.000)	4.97 (0.000)	5.00 (0.000)	5.01 (0.000)	5.01 (0.000)	4.87 (0.002)
Formaldehyde	1^1A_2	$n \rightarrow \pi^*$	3.52 (0.000)	3.47 (0.000)	3.54 (0.000)	3.52 (0.000)	3.50 (0.000)	3.88 (0.000)
	2^1A_1	$\pi \rightarrow \pi^*$	8.66 (0.490)	8.51 (0.483)	8.75 (0.517)	8.74 (0.501)	8.67 (0.491)	9.30 (0.374)
Formamide	1^1A"	$n \rightarrow \pi^*$	5.48 (0.002)	5.46 (0.002)	5.54 (0.002)	5.48 (0.002)	5.46 (0.002)	5.63 (0.001)
	$2^1A'$	$\pi \rightarrow \pi^*$	7.76 (0.579)	7.68 (0.577)	7.77 (0.605)	7.82 (0.588)	7.78 (0.581)	7.44 (0.371)
Imidazole	$2^1A'$	$\pi \rightarrow \pi^*$	6.45 (0.382)	6.38 (0.381)	6.81 (0.414)	6.66 (0.398)	6.54 (0.390)	6.19 (0.088)
	1^1A"	$n \rightarrow \pi^*$	6.50 (0.003)	6.46 (0.003)	6.73 (0.003)	6.61 (0.003)	6.54 (0.003)	6.81 (0.005)
Norbornadiene	1^1A_2	$\pi \rightarrow \pi^*$	4.60 (0.000)	4.48 (0.000)	5.04 (0.000)	4.86 (0.000)	4.70 (0.000)	5.34 (0.000)
	1^1B_2	$\pi \rightarrow \pi^*$	5.72 (0.299)	5.59 (0.296)	6.26 (0.313)	6.04 (0.304)	5.86 (0.300)	6.11 (0.029)
p-Benzoquinone	1^1B_{1g}	$n \rightarrow \pi^*$	2.35 (0.000)	2.17 (0.000)	2.40 (0.000)	2.33 (0.000)	2.27 (0.000)	2.78 (0.000)
	1^1B_{1u}	$\pi \rightarrow \pi^*$	5.02 (1.565)	4.98 (1.572)	5.56 (1.758)	5.42 (1.683)	5.26 (1.635)	5.29 (0.558)
Propanamide	1^1A"	$n \rightarrow \pi^*$	5.28 (0.004)	5.25 (0.004)	5.60 (0.004)	5.45 (0.004)	5.37 (0.004)	5.72 (0.001)
	$2^1A'$	$\pi \rightarrow \pi^*$	7.42 (0.492)	7.35 (0.495)	7.73 (0.539)	7.66 (0.511)	7.55 (0.502)	7.20 (0.108)
Pyrazine	1^1B_{3u}	$n \rightarrow \pi^*$	4.21 (0.008)	4.13 (0.008)	4.28 (0.008)	4.22 (0.008)	4.18 (0.008)	3.95 (0.008)
	1^1B_{2u}	$\pi \rightarrow \pi^*$	6.37 (0.490)	6.32 (0.486)	6.93 (0.518)	6.63 (0.504)	6.46 (0.496)	4.64 (0.067)
Pyridazine	1^1B_1	$n \rightarrow \pi^*$	3.44 (0.008)	3.34 (0.007)	3.62 (0.008)	3.53 (0.008)	3.46 (0.007)	3.78 (0.007)
	2^1A_1	$\pi \rightarrow \pi^*$	6.58 (0.618)	6.50 (0.609)	7.19 (0.688)	6.89 (0.654)	6.70 (0.634)	5.18 (0.014)
Pyridine	1^1B_1	$n \rightarrow \pi^*$	4.62 (0.005)	4.52 (0.005)	4.77 (0.005)	4.69 (0.005)	4.63 (0.005)	4.59 (0.006)
	1^1B_2	$\pi \rightarrow \pi^*$	6.39 (0.517)	6.33 (0.513)	6.96 (0.550)	6.67 (0.534)	6.50 (0.525)	4.85 (0.022)
Pyrimidine	1^1B_1	$n \rightarrow \pi^*$	4.44 (0.007)	4.33 (0.007)	4.58 (0.007)	4.50 (0.007)	4.44 (0.007)	4.55 (0.007)
	1^1A_2	$n \rightarrow \pi^*$	5.96 (0.000)	5.88 (0.000)	6.11 (0.000)	6.03 (0.000)	5.98 (0.000)	4.91 (0.000)
	1^1B_2	$\pi \rightarrow \pi^*$	6.72 (0.614)	6.64 (0.606)	7.32 (0.683)	7.03 (0.650)	6.84 (0.630)	5.44 (0.022)
	2^1A_1	$\pi \rightarrow \pi^*$	6.79 (0.536)	6.69 (0.532)	7.07 (0.562)	6.99 (0.549)	6.87 (0.541)	6.95 (0.038)
s-Tetrazine	1^1B_{3u}	$n \rightarrow \pi^*$	2.65 (0.012)	2.56 (0.011)	2.71 (0.012)	2.66 (0.012)	2.62 (0.011)	2.24 (0.009)
	1^1A_u	$\pi \rightarrow \pi^*$	5.93 (0.000)	5.90 (0.000)	5.20 (0.000)	5.94 (0.000)	5.92 (0.000)	3.48 (0.000)
Thymine	1^1A"	$n \rightarrow \pi^*$	4.94 (0.003)	4.85 (0.003)	4.85 (0.002)	4.86 (0.002)	4.86 (0.002)	4.82 (0.000)
	$2^1A'$	$\pi \rightarrow \pi^*$	5.42 (0.782)	5.35 (0.777)	5.75 (0.791)	5.63 (0.799)	5.52 (0.796)	5.20 (0.222)
Uracil	1^1A"	$n \rightarrow \pi^*$	4.80 (0.002)	4.72 (0.002)	4.67 (0.002)	4.70 (0.002)	4.72 (0.002)	4.80 (0.000)
	$2^1A'$	$\pi \rightarrow \pi^*$	5.48 (0.766)	5.42 (0.758)	5.80 (0.594)	5.69 (0.794)	5.58 (0.789)	5.35 (0.224)
		MD:	0.11	0.03	0.34	0.26	0.17	–
		MAD:	0.54	0.55	0.60	0.57	0.55	–
		RMSD:	0.75	0.76	0.85	0.81	0.77	–
		SD:	0.75	0.77	0.79	0.78	0.76	–
		MAX:	2.45	2.42	2.29	2.46	2.44	–

[a] Best estimate energy value from Ref. S6 (CCSD value for oscillator strength). [b] Structure and reference values (SCS-CC2/aug-cc-pVDZ) from Ref. S5.

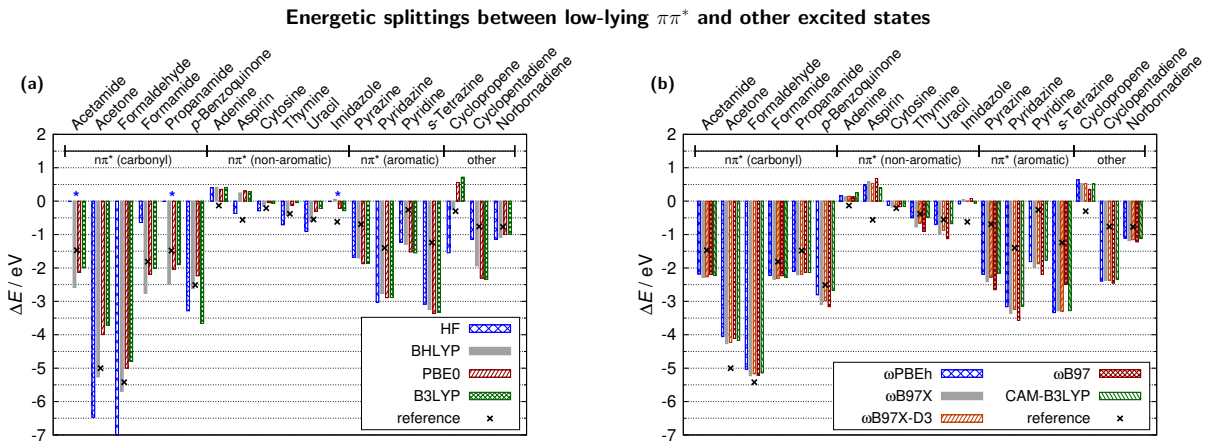

Figure S7: Excited state energy splittings for the excited states given in Tables S8 and S9 (pyrimidine, which has four states, is not included in this figure). For simplicity, pyrimidine is ignored here. Global hybrid functionals are grouped in a), while range-separated hybrids are in grouped in b) (see Tables S8 and S9 for details)

1.5 Standard *hh*-TDA vs FOMO-*hh*-TDA

In Figure S8, we report a comparison of standard *hh*-TDA and FOMO-*hh*-TDA for vertical excitation energies on a benchmark set comprised of the push-pull-type and the local excitation sets (Figures S3 and S5) with cyclopropenone excluded, as it appears to be an outlier for FOMO-*hh*-TDA in combination with any density functional approximation. The ωB97X and BHLYP functionals are employed for both flavors of *hh*-TDA and the def2-SV(P) basis set is used throughout. Overall, the functionals perform similarly for with both choices of orbital generation, with BHLYP improving both in systematic and nonsystematic errors when combined with the FOMO-*hh*-TDA approach. The most drastic improvement is seen for the carbonyl-type systems (and imidazole), for which incorrect orbital occupation was observed for the (N+2) reference (indicated by an asterisk, see Ref. S3). Here, the use of orbitals from the N-electron FON SCF calculation completely remedies this issue and the $\pi\pi^*$ orbital is in fact the highest occupied orbital. For the other systems, only small and system-specific changes are observed. Hence, we suggest that either orbital choice can be chosen at the discretion of the user based on benchmarking for the system of interest.

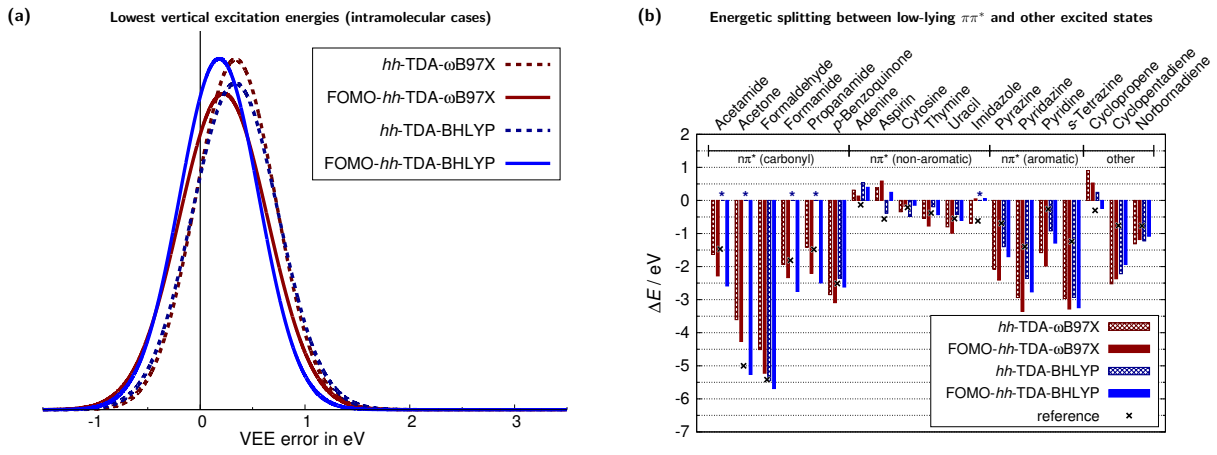

Figure S8: Comparison of *hh*-TDA employing orbitals from an (N+2)-electron SCF reference (labeled *hh*-TDA) or an N-electron FON SCF calculation (labeled FOMO-*hh*-TDA) for the ωB97X and BHLYP functionals. The def2-SV(P) basis set has been used throughout. a) The Gaussian distribution curves visualize the error for the calculation of vertical excitation energies (VEEs). The Gaussian centers correspond to the respective mean deviation (MD), while the standard deviation (SD) is used for the Gaussian width. b) State splittings between low-lying $\pi\pi^*$ and other states (mostly $n\pi^*$). Overall, comparable performance with either orbital choice is observed. Statistics for this set are as follows (in eV). BHLYP (N+2): MD = 0.33, SD = 0.41; ωB97X (N+2): MD = 0.34, SD = 0.38; BHLYP (FON SCF): MD = 0.18, SD = 0.38; ωB97X (FON SCF): MD = 0.22, SD = 0.42.

2 Additional Details for Azobenzene Studies

2.1 Dihedral scans

In addition to the MS-CASPT2 (10 electrons in 8 orbitals active space) scan presented in Figure 5 of the main text, two additional reference calculations can be observed below. In addition to strong agreement with our own MS-CASPT2 calculations, the FOMO-*hh*-TDA-BHLYP/def2-SVP relaxed scan performed in our work benchmarks well against previous results at the same MS-CASPT2 level of theory by other researchers (S9)[S9] and results computed here at the DFT-MRCI-BHLYP/def2-SVP level of theory (S10).

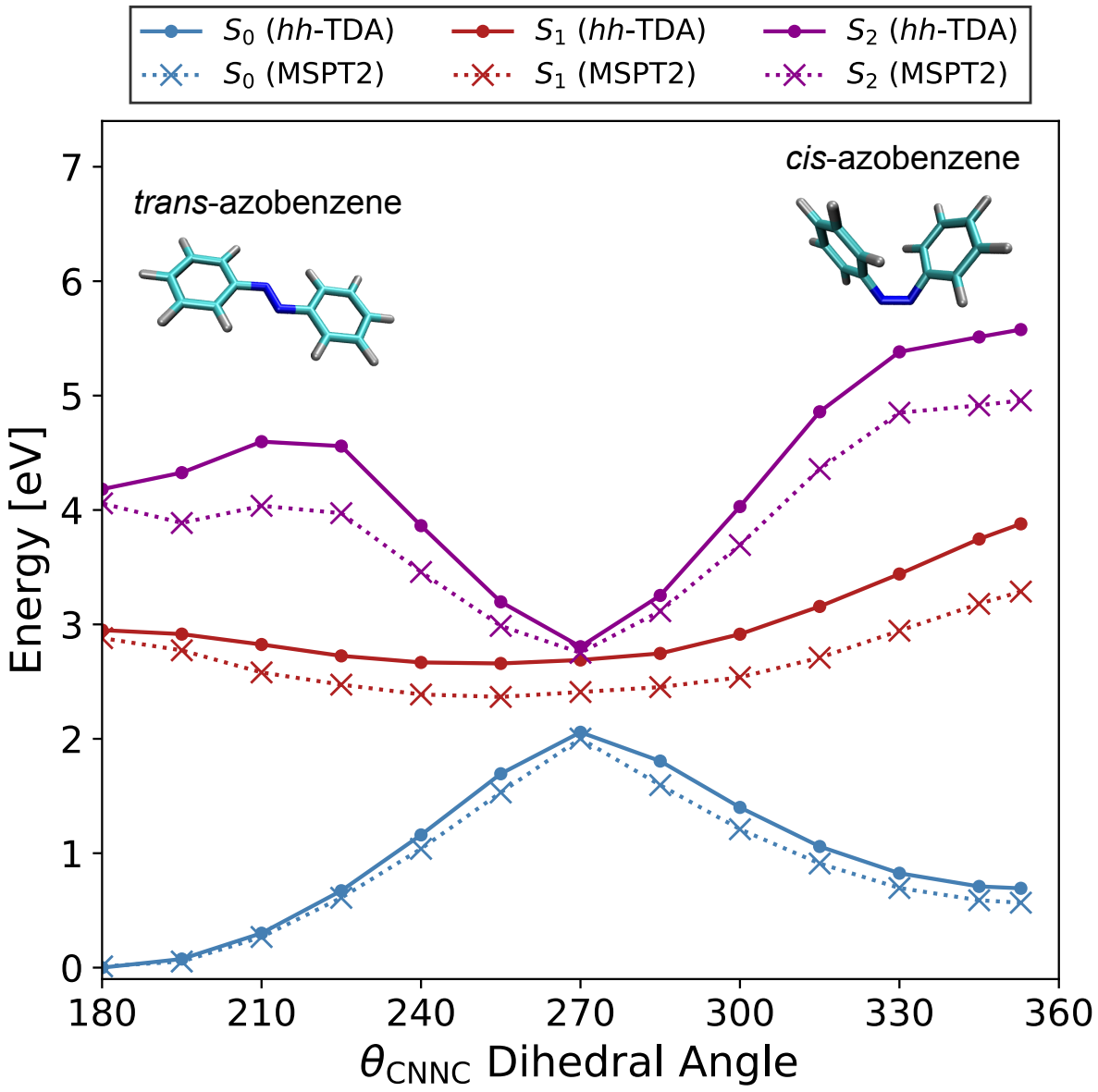

Figure S9: Relaxed scan of azobenzene along fixed θ_{CNNC} dihedral angle values between the *trans* and *cis* conformations (molecular structures shown as insets) using FOMO-*hh*-TDA-BHLYP/def2-SVP (the unconstrained degrees of freedom were relaxed on the S_0 surface). A scan computed by Casellas et al.[S9] at the MS-CASPT2/6-31G(d) (10 electron, 8 orbital active space) level of theory on top of DFT optimized geometries is included for comparison.

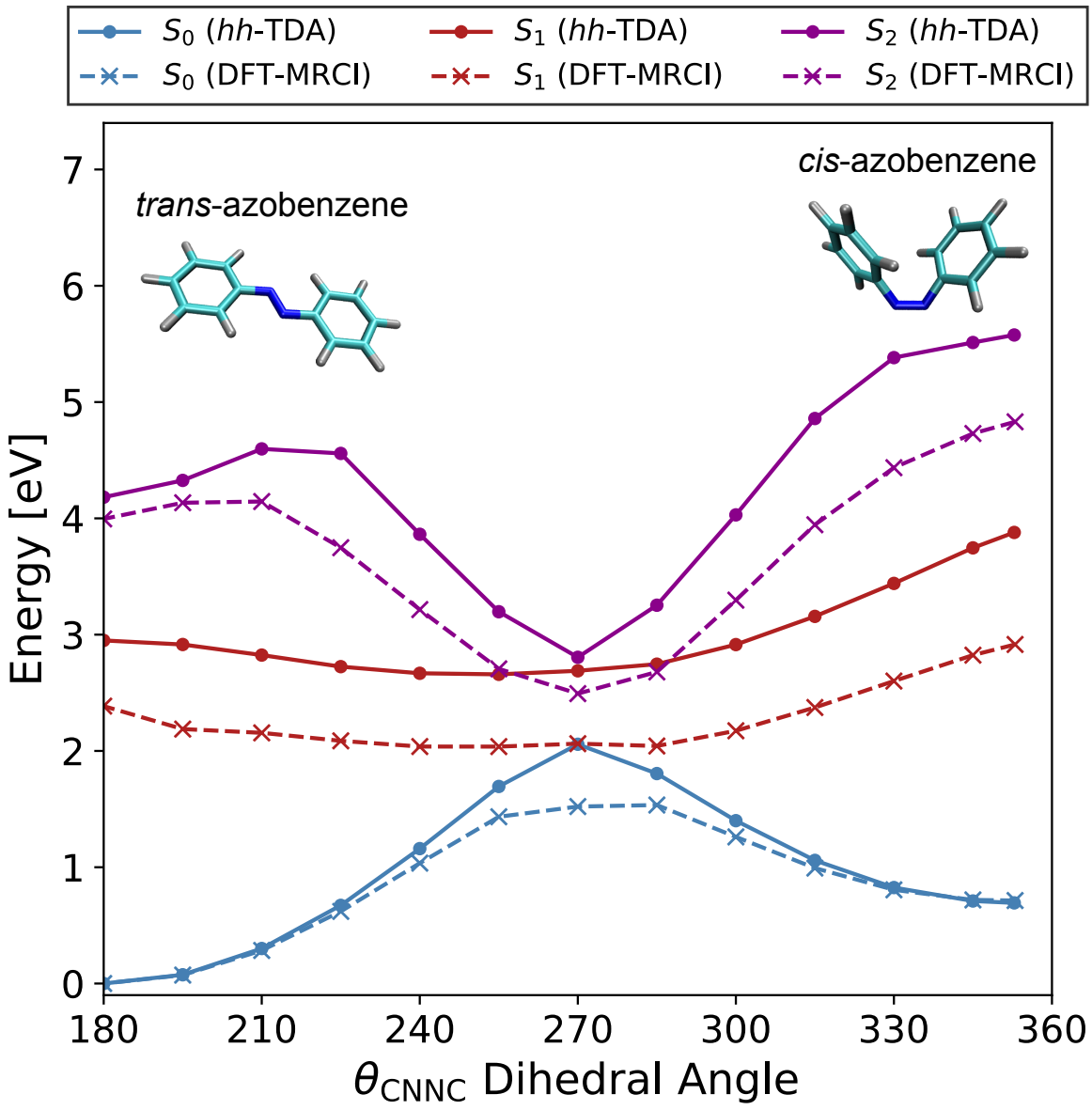

Figure S10: Relaxed scan of azobenzene along fixed θ_{CNNC} dihedral angle values between the *trans* and *cis* conformations (molecular structures shown as insets) using FOMO-*hh*-TDA-BHLYP/def2-SVP (the unconstrained degrees of freedom were relaxed on the S_0 surface). For comparison to a reference-level method, DFT-MRCI[S10,S11] single point calculations using the BHLYP functional (in combination with Turbomole)[S12,S13] are computed on the FOMO-*hh*-TDA optimized geometries.

2.2 Azobenzene AIMS-FOMO-*hh*-TDA-BHLYP/def2-SVP dynamics with d-functions excluded

Nonadiabatic dynamics simulations of azobenzene following excitation to the nπ excited state have previously[S14–S16] been performed by semiempirical methods, such as the OM2/MRCI[S17] methods that employ a minimal basis set (i.e., excluding d-functions). For this reason, we have repeated our azobenzene simulations to also exclude the d-functions in the basis set. To do this, we use the AIMS method with energies, gradients and nonadiabatic couplings obtained at the FOMO-*hh*-TDA-BHLYP level of theory with the def2-SVP basis set modified to exclude d-functions, referenced herein as def2-SVP(-d). We use the same 40 initial conditions as for the azobenzene simulations using the full def2-SVP basis set reported in the main text. The AIMS simulations are continued until more than 98% of the population has decayed to the ground state or until 750 fs. 150 additional trajectory basis functions are spawned from the initial 40 for a total of 190 simulated TBFs.

Population dynamics for the simulations using the def2-SVP(-d) basis set are reported in S11. The lifetime of the S_1 state is extended by the exclusion of the d-functions. Meanwhile, the excited state decay pathways are reported in S12. The use of the def2-SVP(-d) basis set decreases the proportion of the excited state that decays through the unreactive pathway and biases the dynamics toward the reactive pathway, which requires more time and thus extends the excited state lifetime overall. The inclusion of d-functions in the full def2-SVP basis set used in our study thus explains the shorter excited state lifetime in our simulations in comparison to those reported in previous studies.[S14–S16]

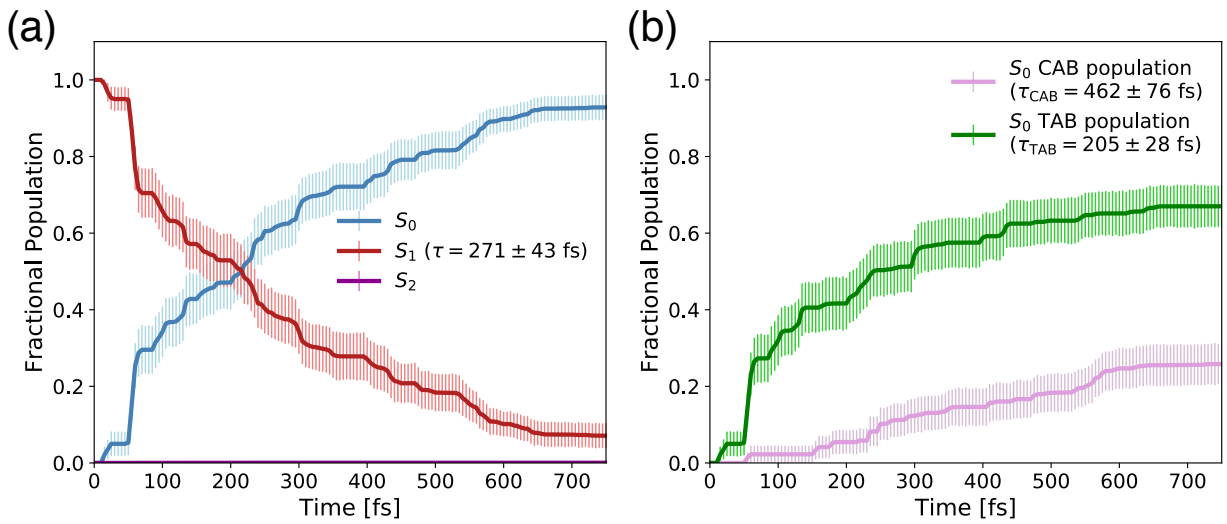

Figure S11: **(a)** Decay of the excited state population and the rise of ground state population (solid curves) from the AIMS simulations of photoexcited TAB described at the FOMO-*hh*-TDA-BHLYP/def2-SVP(-d) level of theory. The decay time of the first excited state is given by an exponential fit to be $\tau = 271 \pm 43$ fs. This is longer than the lifetime of $\tau = 197 \pm 60$ fs reported in Figure 6a of the main text for the simulations with d-functions included. The reported error in the population decay and in the excited state lifetime represent one standard error computed by bootstrapping. **(b)** Rise of the CAB (purple) and TAB (green) photoproducts. 70% of the ground state population recovered is of the trans isomer, while the remaining 30% is of the isomerized cis isomer. This can be contrasted with quantum yields of 81% and 19%, respectively, in the dynamics using the full def2-SVP basis set (Figure 6b).

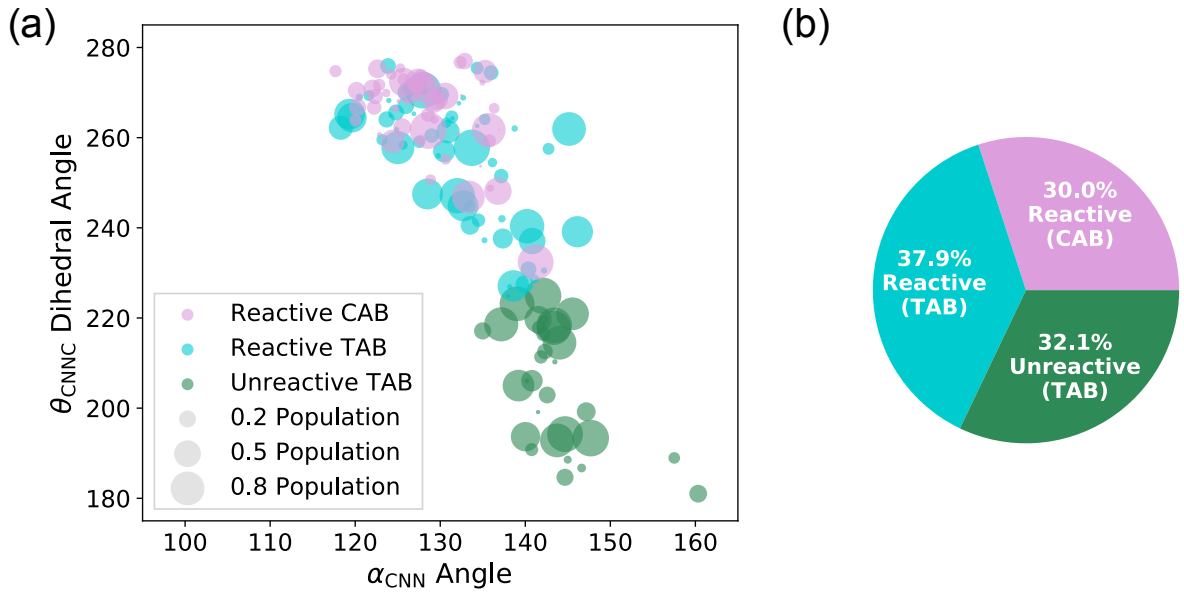

Figure S12: **(a)** Scatter plot of the intersection/spawning geometries placed by the larger α_{CNN} angle and the θ_{CNNC} dihedral angle with the size of each point representing the population transferred from S_1 to S_0 by the spawning geometry in the AIMS dynamics of azobenzene with FOMO-*hh*-TDA-BHLYP/def2-SVP(-d). There are still two distinct classes of intersection geometries here separated by the θ_{CNNC} dihedral angle value of 225°. The unreactive class of intersection geometries is in green and the reactive class is a union of the blue and purple points. The reactive class is subdivided further into reactive intersections that yield the TAB (blue) and CAB (purple) photoproducts. **(b)** The main effect of omitting the d-functions in the basis set is observed in the proportion of population transfer mediated by these reaction pathways, here in a pie chart. 32.1% of the population transfer occurs through the unreactive pathway, 37.9% occurs through the reactive pathway but generates the TAB photoproduct, and 30.0% occurs through the reactive pathway and generates CAB. This is compared to 45.4%, 35.5%, and 19.1%, respectively, in the dynamics results presented in the main text for which the full def2-SVP basis set is used (Figure 7b).

References

(S1) Ufimtsev, I. S.; Martínez, T. J. Quantum Chemistry on Graphical Processing Units. 2. Direct Self-Consistent-Field Implementation. *J. Chem. Theory Comput.* **2009**, *5*, 1004–1015.

(S2) Ufimtsev, I. S.; Martínez, T. J. Quantum Chemistry on Graphical Processing Units. 1. Strategies for Two-Electron Integral Evaluation. *J. Chem. Theory Comput.* **2008**, *4*, 222–231.

(S3) Bannwarth, C.; Yu, J. K.; Hohenstein, E. G.; Martínez, T. J. Hole–hole Tamm–Dancoff-approximated density functional theory: A highly efficient electronic structure method incorporating dynamic and static correlation. *The Journal of Chemical Physics* **2020**, *153*, 024110.

(S4) Risthaus, T.; Hansen, A.; Grimme, S. Excited States Using the Simplified Tamm-Dancoff-Approach for Range-Separated Hybrid Density Functionals: Development and Application. *Phys. Chem. Chem. Phys.* **2014**, *28*, 14408–14419.

(S5) Grimme, S.; Bannwarth, C. Ultra-fast computation of electronic spectra for large systems by tight-binding based simplified Tamm-Dancoff approximation (sTDA-xTB). *J. Chem. Phys.* **2016**, *145*, 054103.

(S6) Schreiber, M.; Silva-Junior, M. R.; Sauer, S. P. A.; Thiel, W. Benchmarks for electronically excited states: CASPT2, CC2, CCSD, and CC3. *J. Chem. Phys.* **2008**, *128*, 134110.

(S7) Weigend, F.; Ahlrichs, R. Balanced basis sets of split valence, triple zeta valence and quadruple zeta valence quality for H to Rn: Design and assessment of accuracy. *Phys. Chem. Chem. Phys.* **2005**, *7*, 3297–3305.

(S8) Schäfer, A.; Horn, H.; Ahlrichs, R. *J. Chem. Phys.* **1992**, *97*, 2571–2577.

(S9) Casellas, J.; Bearpark, M. J.; Reguero, M. Excited-State Decay in the Photoisomerisation of Azobenzene: A New Balance between Mechanisms. *ChemPhysChem* **2016**, *17*, 3068–3079.

(S10) Grimme, S.; Waletzke, M. *J. Chem. Phys.* **1999**, *111*, 5645.

(S11) Marian, C. M.; Heil, A.; Kleinschmidt, M. The DFT/MRCI method. *WIREs Computational Molecular Science* **2019**, *9*, e1394.

(S12) TURBOMOLE V6.4 2012, a development of University of Karlsruhe and Forschungszentrum Karlsruhe GmbH, 1989-2007, TURBOMOLE GmbH, since 2007; available from
`http://www.turbomole.com`.

(S13) Furche, F.; Ahlrichs, R.; Hättig, C.; Klopper, W.; Sierka, M.; Weigend, F. Turbomole. *WIREs Comput. Mol. Sci.* **2014**, *4*, 91–100.

(S14) Gámez, J. A.; Weingart, O.; Koslowski, A.; Thiel, W. Cooperating Dinitrogen and Phenyl Rotations in trans-Azobenzene Photoisomerization. *Journal of Chemical Theory and Computation* **2012**, *8*, 2352–2358, PMID: 26588968.

(S15) Ciminelli, C.; Granucci, G.; Persico, M. The Photoisomerization Mechanism of Azobenzene: A Semiclassical Simulation of Nonadiabatic Dynamics. *Chemistry – A European Journal* **2004**, *10*, 2327–2341.

(S16) Toniolo, A.; Ciminelli, C.; Persico, M.; Martínez, T. J. Simulation of the photodynamics of azobenzene on its first excited state: Comparison of full multiple spawning and surface hopping treatments. *The Journal of Chemical Physics* **2005**, *123*, 234308.

(S17) Koslowski, A.; Beck, M. E.; Thiel, W. Implementation of a general multireference configuration interaction procedure with analytic gradients in a semiempirical context

using the graphical unitary group approach. *Journal of Computational Chemistry* **2003**, *24*, 714–726.